Supporting Information

Construction of multi-layer Pt-based self-supporting catalyst for high-current-density hydrogen evolution reaction

Suhui Chen [a, b], Bowen Lu [a, b], Wei Wang [a], Siyu Yang [a, b], Haohao Gao [a, b], Haiwei Xu [a, b], Bingxin Li [a], Zile Hua [a, b] and Jian Huang [a, *]

Author ADDRESS: [a] State Key Laboratory of High Performance Ceramics and Superfine Microstructure, Shanghai Institute of Ceramics Chinese Academy of Sciences, 1295 Dingxi Road, Shanghai, China. [b] Centre of Materials Science and Optoelectronics Engineering, University of Chinese Academy of Sciences, Beijing, China.

Experimental Section

Chemical

Nickel sulfate hexahydrate ($NiSO_4·6H_2O$), Cobalt sulfate heptahydrate ($CoSO_4·7H_2O$), copper sulfate ($CuSO_4$), Chloroplatinic Acid (H_2PtCl_6), sodium hypophosphite hydrate ($NaH_2PO_2·H_2O$), Sodium borohydride ($NaBH_4$), ammonium sulfate ($(NH_4)_2SO_4$), Sodium citrate ($Na_3C_6H_5O_7$), Potassium sodium tartrate ($KNaC_4H_4O_6$), Ethylenediamine (EDA), Polyethylene glycol (PEG) hydrochloric acid (HCl) and sodium hydroxide (NaOH) were purchased from Sigma-Aldrich and Adamas. All chemicals are of analytical grade and were used without any further purification.

Preparation of NiP/FP

The chemicals used in the synthesis process are all analytical grades and added without further treatment. Initially, the filter paper (FP) was activated via two steps to provide active sites pivotal for the electroless plating. The activation step generates Ni^0, which serves as the foundation for initiating redox reactions in the electroless plating solution. The FP was dried in a vacuum oven to avoid further oxidation. Subsequently, cleaned NF was dipped in 0.3 M $NiSO_4$ and 0.3 M $NaBH_4$ solutions for 5 min, respectively, and then transferred into the plating solution. The electroless deposition of NiP/FP alloy is carried out in a 200 mL solution containing 0.01 mol $NiSO_4·6H_2O$, 0.04 mol $NaH_2PO_2·H_2O$, 0.02 mol $Na_3C_6H_5O_7·2H_2O$, 0.076 mol $KNaC_4H_4O_6·4H_2O$, 0.03 mol

$(NH_4)_2SO_4$. The temperature of the electroless plating solution was raised to 60 °C, and the deposition time was controlled to be 90 min. After the electroless plating, the NiP/FP electrode material was rinsed with deionized water for later use.

Preparation of Cu-NiP/FP

The prepared NiP/FP electrode material was immersed in the plating solution at 65 °C for 20 min, which is composed of 0.04 mol/L $CuSO_4$, 0.01 mol/L $NiSO_4$, 0.48 mol/L H_3BO_3, 0.34 mol/L NaH_2PO_2, and 1 g/L PEG. After the electroless plating, the NiP/FP electrode material was rinsed with deionized water for later use.

Preparation of Pt-Cu-NiP/FP

For the synthesis of Pt-Cu-NiP/FP electrode, 10 mL H_2PtCl_6 (1 mg/mL), 4 g NaOH, 2 mL EDA, 0.05 g $NaBH_4$ were added into 100 mL deionized water and stirred to form homogeneous electroless plating solution, and as-prepared was immersed into a 100 mL freshly prepared electroless plating solution at 40 °C for 2h. After 2 hours of reaction, the as-synthesized Pt-Cu-NiP/FP was washed with deionized water and dried overnight.

Preparation of Pt/FP, Pt/FP-200-1, Pt/FP-200-3 and Pt-Cu-NiP/FP-200-1, Pt-Cu-NiP/FP-200-3.

The synthesis of Pt/FP was fabricated using a similar strategy without Cu and NiP layers. The Pt/FP was placed in the middle of the pipe furnace and heated at 200 °C. The time was changed to 1 h and 3 h; other conditions remained unchanged. Pt/FP-200-1 and Pt/FP-200-3 were obtained, respectively. The Pt-Cu-NiP/FP-200-1 and Pt-Cu-NiP/FP-200-3 were prepared by the same heat treatment.

Preparation of Pt/C @ FP

5 mg 20% Pt/C (M.W. 195.08, Pt 20%, Hesen) was dispersed in 220 μL of water / ethanol / 5 wt% Nafion (V / V / V = 100 : 100 : 20) and sonicated for 30 min. Then the catalyst ink was pipetted onto the FP with a mass loading of approximately 0.46 mg cm^{-2} to prepare Pt/C @ a-FP according to the calculation of weight gain of the a-FP.

Physical Characterizations. X-ray photoelectron spectroscopy (XPS, EscaLab 250Xi) was performed to obtain the surface species and chemical valences. Moreover, the depth XPS with the Ar^+ etching was applied to further investigate the surface species and chemical valences of inner catalyst layer. Scanning electron microscopy (SEM, Japan S-4800) and transmission electron microscopy (TEM, FEI-Talos F200X) was applied to analyze the morphology and phase changes of

catalysts before and after the reconstruction process. Powder X-ray diffraction (XRD, Bruker D8-Advance with Cu Kα radiation) patterns were collected to reveal amorphous nature of catalyst. Inductively coupled plasma optical emission spectroscopy (ICP-OES) analysis was carried out with a VARIAN 710ES system. X-ray absorption spectroscopy (XAS) was performed using the BL11B beamlines of the Shanghai Synchrotron Radiation Facility.

Electrochemical Measurements. The electrochemical experiments were tested on a CHI 660E electrochemical workstation using a standard three-electrode system, which the prepared FP, NiP/FP, Cu-NiP/FP, Pt-NiP/FP, and Pt-Cu-NiP/FP as the working electrodes, Hg/HgO as the reference electrode, and a graphite rod as the counter electrode. And all electrochemical environment was in a 1.0 M KOH electrolyte. The potential conversion between the reversible hydrogen electrode (RHE) and the Hg/HgO electrode in the experiment is carried out according to the Nernst equation, as shown in equation (1).

$$E\ (RHE) = E(Hg/HgO) + 0.098\ V + 0.059 \times pH \quad (1)$$

The HER catalytic activity of synthesized electrodes was tested by Linear Sweep Voltammetry (LSV), and a scanning speed of 5 mV s^{-1} was used during the HER test. And, all polarization curves were corrected by iR compensation command. Electrochemical impedance spectroscopy (EIS) was measured in a frequency range from 100 kHz to 0.1 Hz with an amplitude of 5 mV. The EIS patterns contain two types of impedance information, the one is the solution resistance (Rs) and the other is charge transfer resistance (R_{ct}). The stability of synthsized samples was evaluated by amperometric i-t test. The electrochemical active surface area (ECSA) of the prepared samples was calculated with electrochemical double-layer capacitance (C_{dl}). For ECSA analysis, the CV test was carried out with different scan rates from 20 to 100 mV s^{-1} under the non-Faradaic overpotential region. Then the ECSA was estimated based on equation (2)

$$ECSA = C_{dl}/C_s \quad (2)$$

where C_s is the specific capacitance, whose value is reported to be 0.04 mF cm^{-2}.

The normalized current densities (J_{ECSA}) are obtained through dividing by the ECSA, as following equation (3)

$$j_{ECSA} = j/ECSA \quad (3)$$

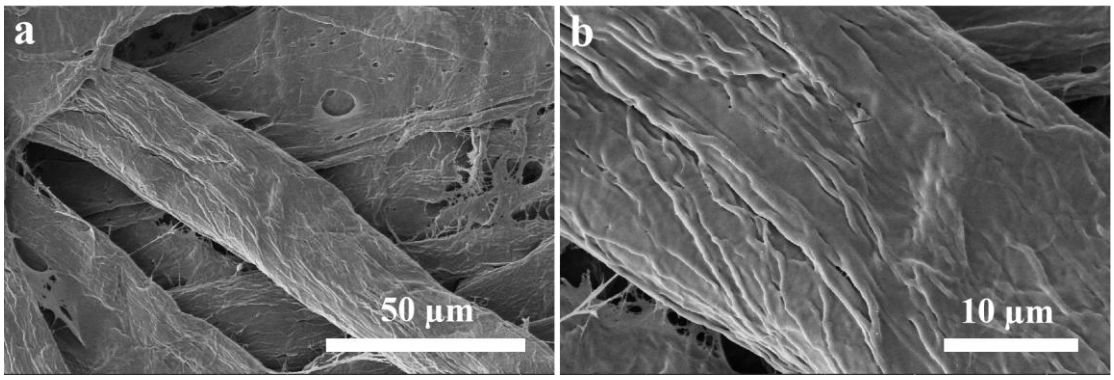

Figure S1 SEM images of pristine FP with different magnifications.

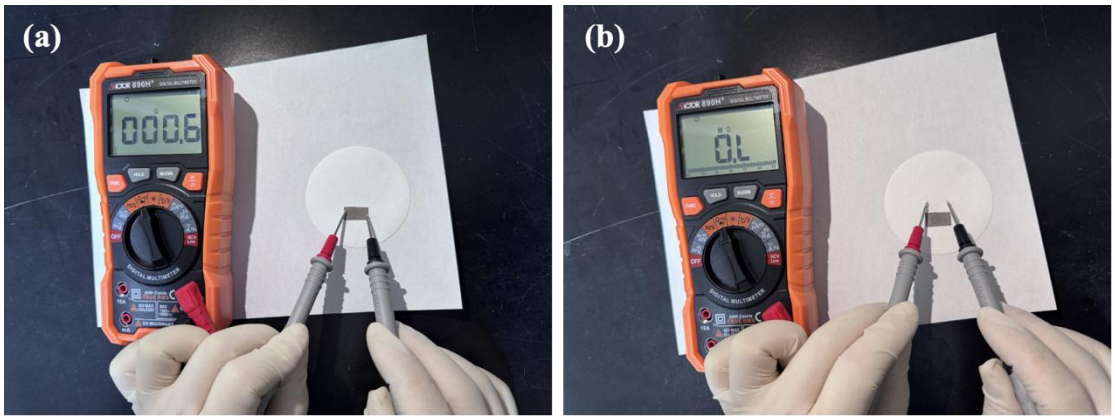

Figure S2 Conductivity of (a) NiP/FP, and (b) FP.

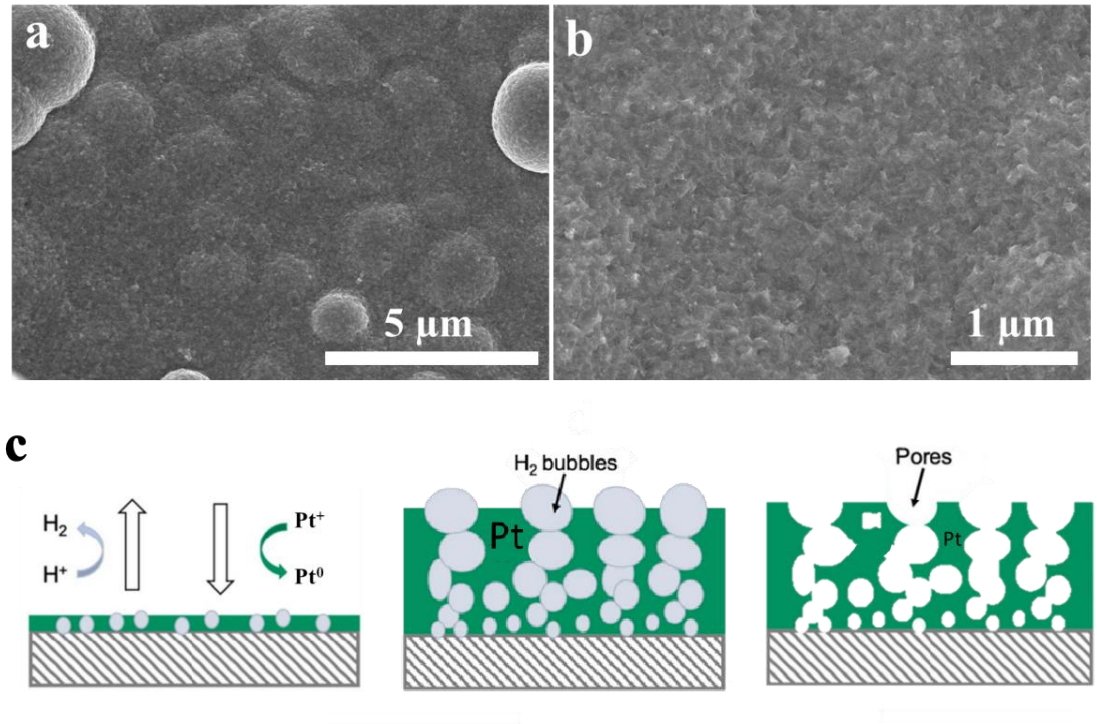

Figure S3 SEM images of (a-b) Pt/FP, (c)Schematic process of the generation of porous Pt.

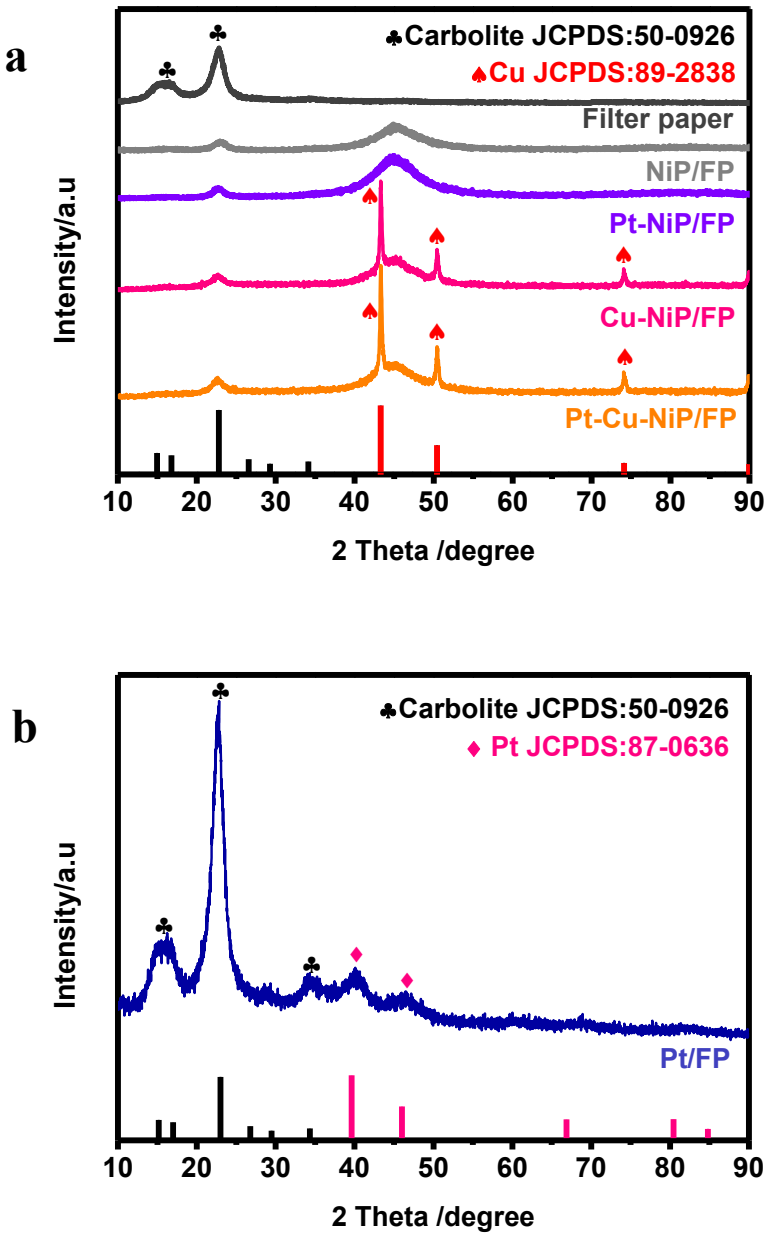

Figure S4 XRD pattern of (a) FP, NiP/FP, Pt-NiP/FP, Cu-NiP/FP, Pt-Cu-NiP/FP (b) Pt/FP.

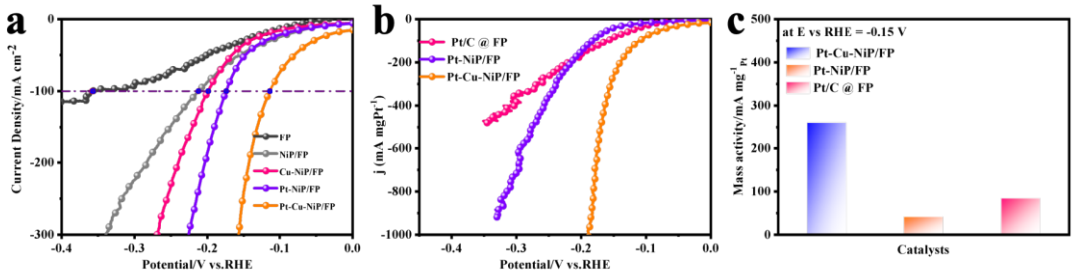

Figure S5 (a)Enlarged view of LSV curves of FP, NiP/FP, Cu-NiP/FP, Pt-NiP/FP, and Pt-Cu-NiP/FP, (b) LSV curves normalized by the mass of Pt for Pt/C @ FP, Pt-NiP/FP, and Pt-Cu-NiP/FP, and (c) Mass activity of the Pt-containing catalysts.

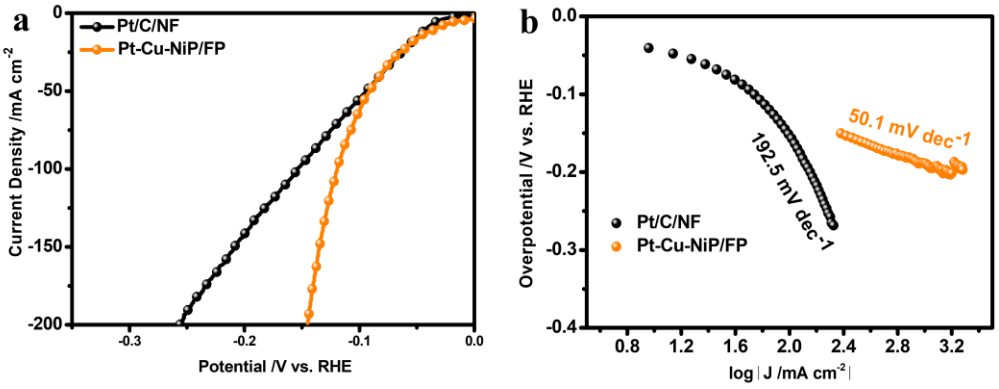

Figure S6 (a) HER polarization curves for Pt/C/NF and Pt-Cu-NiP/FP, and (b) Tafel plots for Pt/C/NF and Pt-Cu-NiP/FP.

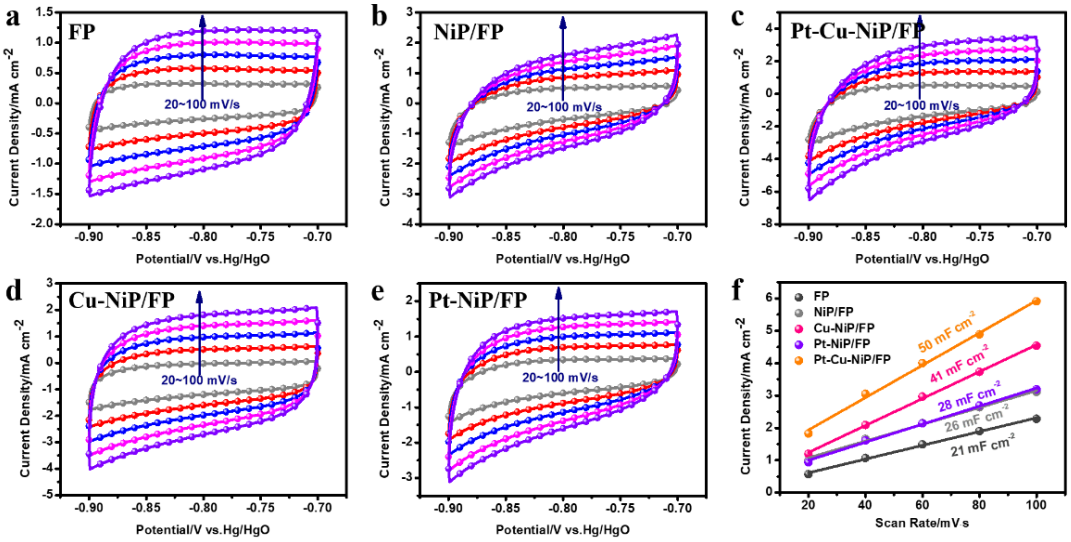

Figure S7 CV for measuring ECSA of as-prepared samples: (a) FP, (b) NiP/FP, (c) Pt-Cu-NiP /FP (d) Cu-NiP/FP (e) Pt-NiP/FP, and (f) C_{dl} values of as-prepared samples for HER.

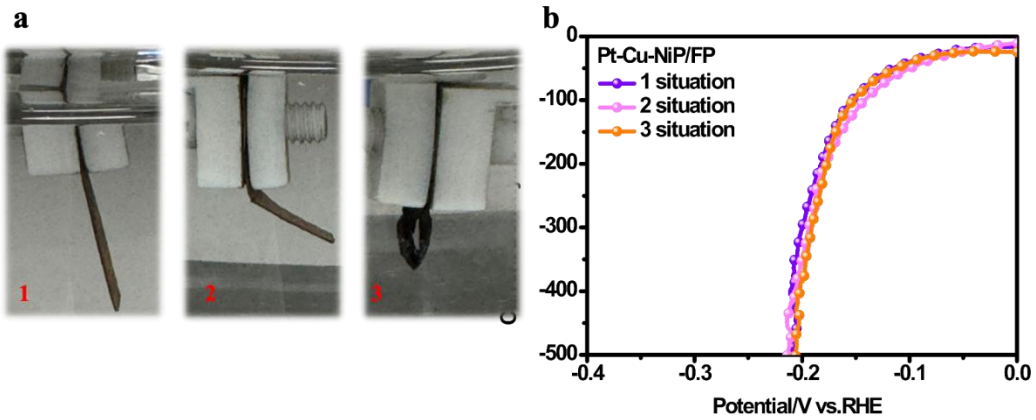

Figure S8 (a) Digital images of Pt-Cu-NiP/FP electrode folded at different situations. (b) Corresponding HER polarization curves of folded Pt-Cu-NiP/FP.

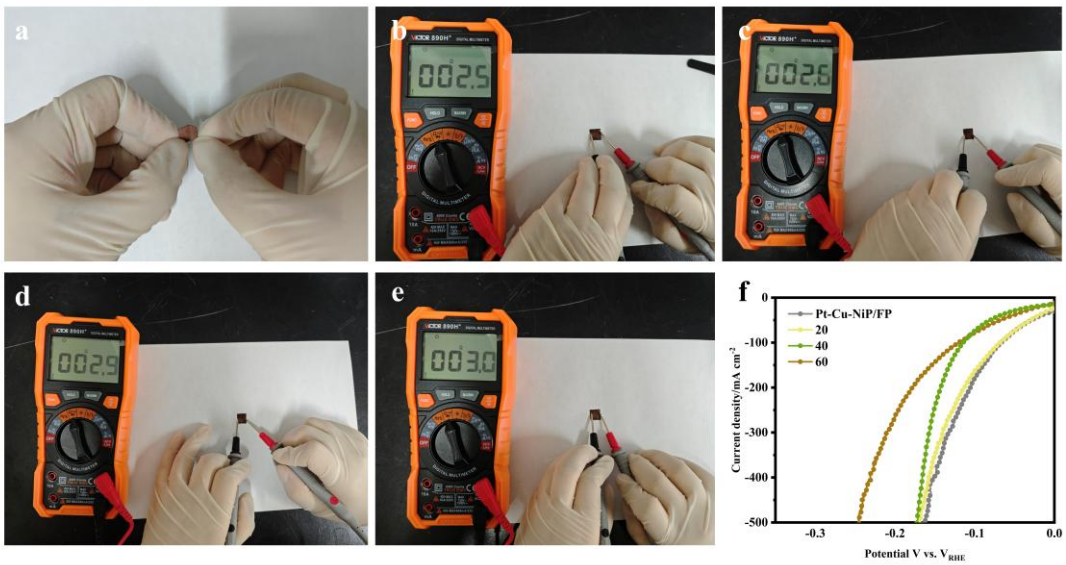

Figure S9 (a) Folded Pt-Cu-NiP/FP after 60 times. (b-f) Surface resistance and LSV curves of original Pt-Cu-NiP/FP and folded samples after 20, 40, 60 times, respectively.

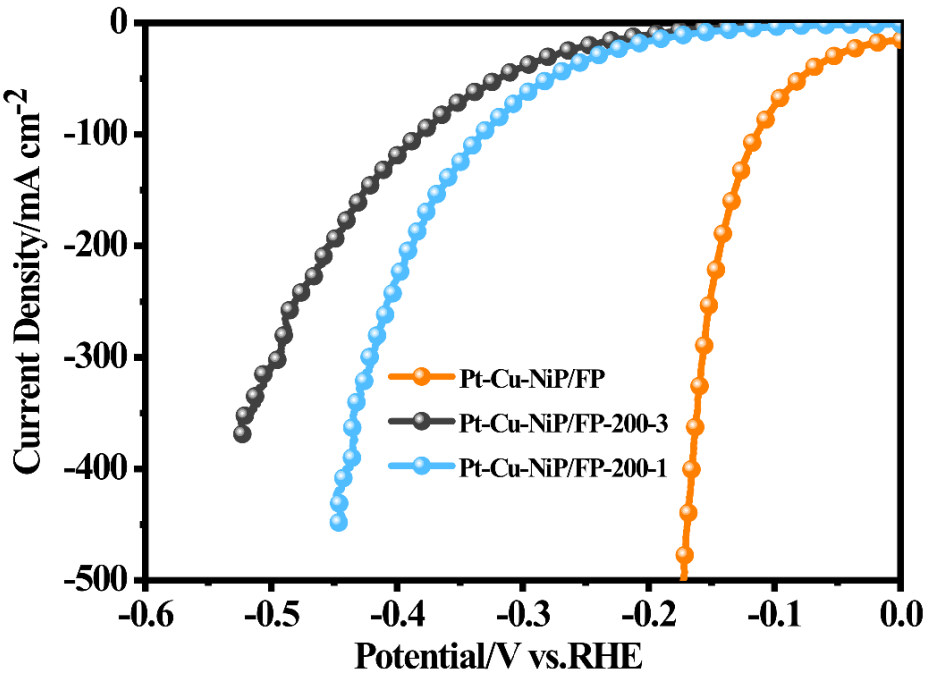

Figure S10 HER curves of Pt-Cu-NiP/FP, Pt-Cu-NiP /FP-200-1, Pt-Cu-NiP /FP-200-3.

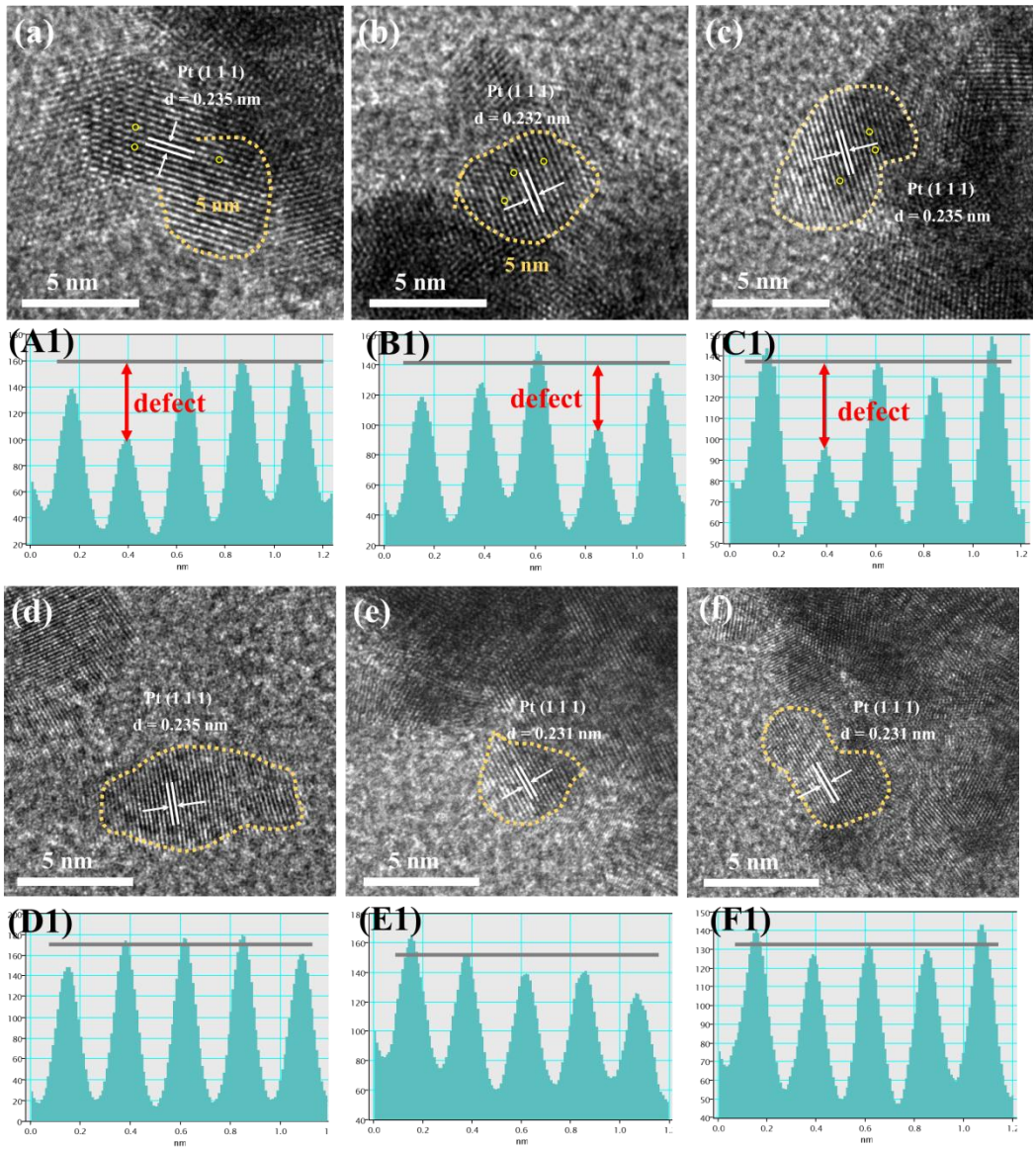

Figure S11 TEM images of (a-c) Pt/FP, (d-f) Pt/FP-200-3 and corresponding TEM software analysis of (A1-C1) Pt/FP, (D1-F1) Pt/FP-200-3.

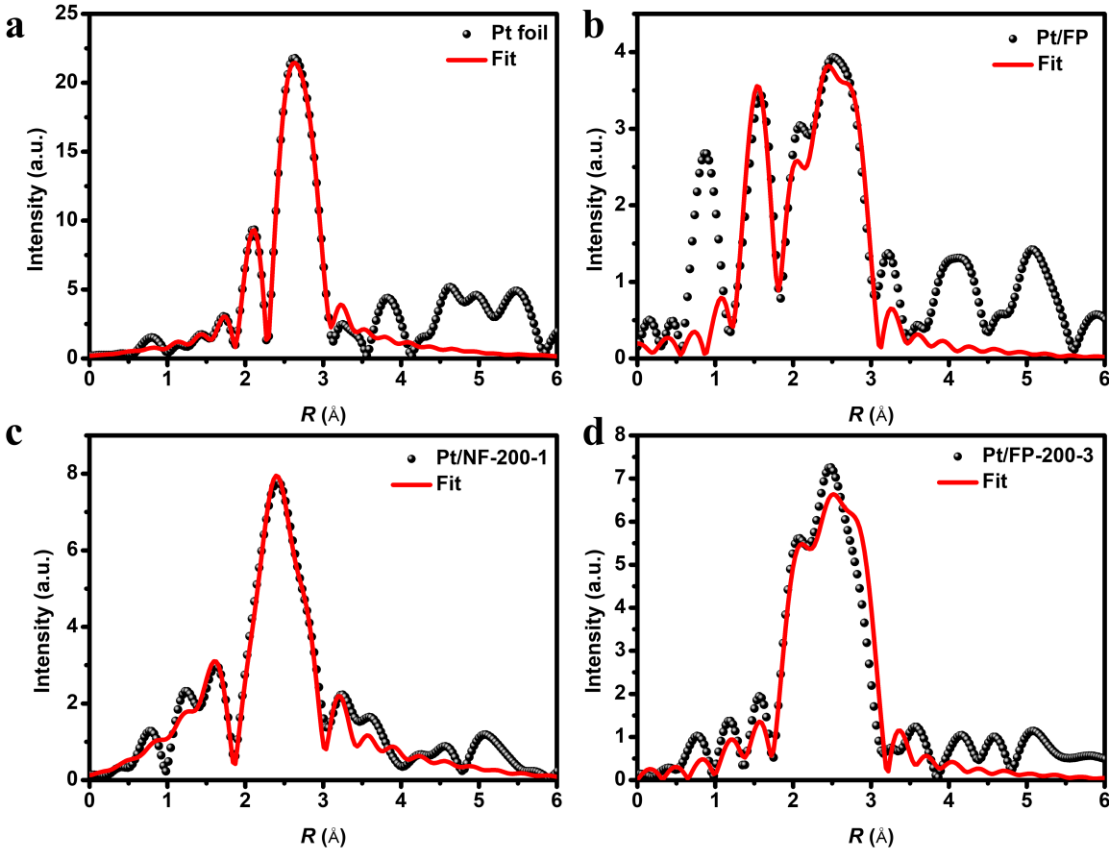

Figure S12 EXAFS fitting results for Pt L3-edge of (a) Pt foil, (b)Pt/FP, (c) Pt/FP-200-1, and (d) Pt/FP-200-3.

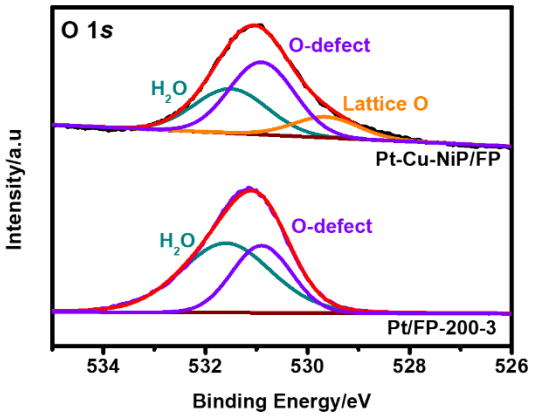

Figure S13 The O 1s XPS spectrum of the Pt/FP-200-3 sample after a 3-hour heat treatment.

Table S1. ICP-OES results of Pt in Pt-Cu-NiP/FP.

Sample	Original plating solution (μg/mL)	After 2 h plating (μg/mL)
Pt-Cu-NiP/FP	18.7	9.5
Pt-NiP/FP	18.7	6.1
pt/FP	18.7	7.0

Table S2 Comparison of HER performance in 1.0 M KOH for Pt-Cu-NiP/FP with other Pt-based catalysts.

Catalyst	Overpotential (mV, j=10 mA cm^{-2})	Tafel slope (mV dec^{-1})	Reference
Pt/NiO/Ni/CNT	117	65	***Nanoscale***, 2020, 12, 14615
0.25-HCM@PtSA	48	76	***Nano Research***, *2025*, 18 (8), 94907671.
PtSAsNi	42	64.8	***Journal of Energy Chemistry***, 2024, 98, 503-511.
Pt/Vo-TiO_2	56	73.5	***Langmuir : the ACS journal of surfaces and colloids***,2023,39(36):
Pt NPs@CF	49	36	***Adv. Funct. Mater***. 2024, 34, 2411283.
Hexagonal-PtNi	65	74	***Nat. Commun.***, 2017, 8, 15131
Pt clusters-MoS_2	94	65.9	***Adv. Funct. Mater.*** 2025, 35, 2423262.
N, Pt-MoS_2	38	39	***Energy Environ. Sci.***, 2022, 15, 1201-1210
Pt-NiCo LDO	92	73	***Adv. Funct. Mater.*** 2024, 34, 2405919.
Pt-Cu-NiP/FP	37	50.1	This work

Table S3 EXAFS fitting parameters at the Pt L3-edge for various samples.

CN, coordination number; R, distance between absorber and backscatter atoms; σ^2, Debye-Waller factor to account for both thermal and structural disorders; ΔE, inner potential correction; R factor indicates the goodness of the fit.

Sample	path	CN	σ^2 (Å)^2	ΔE (eV)	R (Å)	R factor
Pt foil	Pt-Pt	12	0.004	7.5±0.4	2.76±0.01	0.006
Pt/FP	Pt-O	2	0.006	8.0±1.1	2.01±0.06	0.015
	Pt-Pt	9.6±1.2	0.007	8.0±1.1	2.74±0.04	
Pt/FP-200-3	Pt-O	1	0.011	10.4±1.3	1.92±0.02	0.018
	Pt-Pt	11	0.007	10.4±1.3	2.74±0.01	
PtO_2	Pt-O	7±1.0	0.003	9.4±1.7	1.99±0.01	0.013